Soft Matter

Accepted Manuscript

This article can be cited before page numbers have been issued, to do this please use: M. N. Garaga, M. Persson, N. Yaghini and A. Martinelli, *Soft Matter*, 2016, DOI: 10.1039/C5SM02736E.

ROYAL SOCIETY OF CHEMISTRY

www.rsc.org/softmatter

Soft Matter

RSCPublishing

View Article Online
DOI: 10.1039/C5SM02736E

ARTICLE

Local Coordination and Dynamics of a protic Ammonium based Ionic Liquid Immobilized in Nano-Porous Silica Micro-Particles Probed by Raman and NMR Spectroscopy

Cite this: DOI: 10.1039/x0xx00000x

Mounesha N. Garaga,[a] Michael Persson,[a,b] Negin Yaghini[a] and Anna Martinelli*[a]

Received 00th January 201x,
Accepted 00th January 201x

DOI: 10.1039/x0xx00000x

www.rsc.org/

Room temperature ionic liquids confined in a solid material, for example nano-porous silica, are particularly propitious for energy related applications. The aim of this study is to probe the molecular interactions established between the protic ionic liquid diethylmethylammonium methanesulfonate (DEMA-OMs) and silica, where the latter consists in nano-porous micro-particles with pores in the size range of 10 nm. The changes in local coordination and transport properties induced by the nano-confinement of the ionic liquid are investigated by a combination of Raman and solid-state NMR spectroscopy. In particular, one-dimensional (1D) ^{1}H and ^{29}Si, and two-dimensional (2D) ^{29}Si{^{1}H} HETOCR solid-state NMR are combined to identify the sites of interaction at the silica-ionic liquid interface. Pulsed field gradient (PFG) NMR experiments are performed to estimate the self-diffusion of both bulk and nano-confined DEMA-OMs. Complimentary information on the overall coordination and interaction scheme is achieved by Raman spectroscopy. All these advanced experimental techniques reveal to be crucial to differentiate between ionic liquid molecules residing in the inter- or intra-particle domains.

1 Introduction

In the last years the interest in studying room temperature ionic liquids (ILs) has boosted, because of their unique physicochemical properties as compared to organic solvents.[1] For real applications, ILs are even more useful if immobilized in a solid porous matrix, as a means to overcome leakage problems. This immobilization finds applications in catalysis,[2, 3] drug delivery,[4, 5] and sensing,[6] as well as in energy related devices.[7-10] In these contexts, it becomes of pivotal importance to understand the extent to which the physicochemical properties of the ionic liquid change upon confinement, but also to investigate if new properties can emerge as a consequence of the nano-confined state.

Dai *et al.*[11] were pioneering in proposing an alternative method to synthesize silica-based aerogels using an ionic liquid as the solvent, which then lead to the concept of ionogels.[8, 9, 12-15] Recent works on ionogels have shown that these hybrid materials are mechanically[16, 17] and thermally[18, 19] stable, and capable of withstanding temperatures as high as 300 °C. Ionogels based on protic[10, 20] and aprotic[12, 21-23] imidazolium ionic liquids have been extensively studied for applications in for instance the proton exchange membrane (PEM) fuel cell. The nature of interactions at the silica-IL interface determines the physicochemical properties of the ionogel, which may be tuned by changing the chemistry of the silica surface, for example varying it from hydrophilic to hydrophobic.[20, 21] One attempt in this direction has been made by Iacob et al.[21], who have indeed reported an increase in the diffusion coefficient for

[a] *Department of Chemistry and Chemical Engineering, Chalmers University of Technology, 412 96 Gothenburg, Sweden. Email: anna.martinelli@chalmers.se*

[b] *AkzoNobel Pulp and Performance Chemicals AB, Bohus, Sweden.*

Electronic Supplementary Information (ESI) available: 2D solid-state ^{29}Si{^{1}H} HETCOR NMR spectrum of the silica gel with a volume fraction of silica ΦSiO_2 = 0.68, dehydrated at 150 °C for 24 hours. Plot of ^{1}H NMR chemical shifts and FWHM versus ΦSiO_2. Raman spectra of silica gels with ΦSiO_2 varying in the range 0–0.68. Plots of $Ln(I/I_0)$ versus $(\gamma G\delta)^2(\Delta-\delta/3)$ for gels with varying silica content. Plot of the molar conductivity calculated from the self-diffusion data through the Nernst-Einstein relation. Representative I/I_0 vs. G curves for pure DEMA-OMs and a silica gel. Calculation of volume fraction of silica (φSiO_2), percent of pore filling, and conductivity (σ_{NMR}) of silica gels. See DOI: 10.1039/b000000x/

the aprotic ionic liquid 1-hexyl-methylimidazolium hexafluorophosphate (C_6C_1Im-PF_6) when immobilized in silanized silica nano-pores (pore size of 7.5 nm) as compared to untreated nano-pores. If surface interactions are strong enough, the ionic liquid layer closest to the silica surface may display slower diffusional properties, even though this layer has been predicted by molecular dynamic simulations[24] to be only 1-2 nm thick, a result that was almost simultaneously experimentally verified by NMR spectroscopy.[12] Due to surface interactions, this first layer may also display perturbed cation-anion coordinations and a different conformational state.[12, 23, 25] From these considerations, it also turns out that the filling factor, i.e. the portion of the porous volume actually occupied by the ionic liquid, is crucial in determining the transport properties observed for the ionogel. Hence, a higher filling factor would decrease the contribution of surface effects,[23, 26, 27] but possibly also weaken the overall mechanical properties of the ionogel.

Nano-confinement can affect ionic liquid properties other than the self-diffusion, for example the phase behaviour.[28, 29] Some recent works based on the use of differential scanning calorimetry (DSC) or temperature dependent Raman spectroscopy, have revealed that both the glass transition and the melting temperature of imidazolium based ionic liquids can shift or disappear, [25, 30] depending on several factors like pore size, structure of the ionic liquid, and chemistry of the silica's pore wall. A shared conclusion from all the theoretical and experimental works mentioned above is that the ionic liquid at the centre of the pores behaves differently from that directly interacting with the silica pore wall.[13, 23, 31] It turns out that to develop better performing ionogels, in which liquid-like transport properties can be kept despite the nano-confined state, a molecular level understanding of the structure-property relationship must be developed and new strategies to manipulate the nature of surface interactions need to be proposed.

This work contributes to this field with a detailed study, by complementary and advanced spectroscopic techniques, of the effect of pore filling when the protic ionic liquid DEMA-OMs is confined in nano-porous silica micro-particles with a pore diameter of 10 nm. These micro-particles offer a three-dimensionally extended and interconnected nano-porosity, which results in a homogeneous distribution of the ionic liquid also at the macroscopic scale. This is an advantage compared to previously investigated ionogels, whose structure consists of silica domains or aggregates of various size non-uniformly dispersed in the ionic liquid phase (see for instance the TEM image given in the recent work of Nayeri et al.[12]). In the latter scenario, approximations about for instance the available surface area must be done if theoretical models have to be applied to experimental data. DEMA-OMs is non-fluorinated and ammonium based, and thus environmentally more friendly than other ionic liquids investigated before. More specifically, we present results on the molecular proximity of different resonant nuclei at the silica/ionic liquid interface as deduced from multi-dimensional solid-state magic angle spinning (MAS) nuclear magnetic resonance (NMR) spectroscopy. The site and nature of intermolecular interactions are investigated by comparing ^{1}H NMR with Raman spectra, while the mobility of the individual ions is probed by pulsed field gradient (PFG) NMR spectroscopy. This method is very powerful to probe the diffusion of molecules both in the bulk and in restricted domains,[32-34] and for the latter to reveal structural anisotropy.[35] All properties are investigated for a wide range of ionic liquid-to-silica concentrations, i.e. for varying filling factors.

Moreover, being focused on the protic ionic liquid DEMA-OMs, a hot candidate for use as proton conductor in next-generation PEM fuel cells,[36] this work fills the gap between fundamental research on ionogels and their use in real applications. Finally, by virtue of being prepared through a well established synthetic route that allows fine tuning the size and shape of the nano-pores, these silica micro-particles also represent a structurally tuneable model system for basic research on the effects of nano-confinement on any molecular liquid.

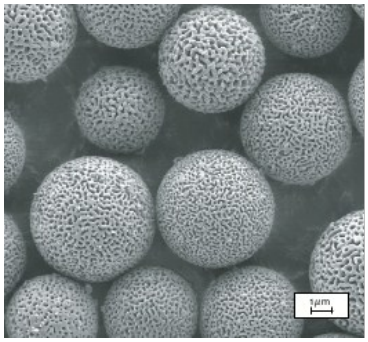

Fig. 1 Typical SEM image of the nano-porous silica micro-particles, here having a diameter ranging between 4-6 um.

2 Experimental Section

2.1 Synthesis of nano-porous silica

The nano-porous silica micro-particles have been synthesized following an established emulsion solvent evaporation procedure that results in tunable pore volume and pore size distributions.[37] Results from Brunauer-Emmett-Teller (BET) analysis reveal that the average pore size of these silica particles is 10 nm and that the surface area is 338 m^2/g. The average particle size is estimated to be 13 μm. A typical SEM image of this type of nano-porous silica micro-particles is given in Figure 1.

2.2 The ionic liquid

The ionic liquid DiEthylMethylAmmonium MethaneSulfonate (DEMA-OMs) was purchased from Iolitec (Germany). Karl Fisher analysis revealed that the as purchased ionic liquid contained 0.07 water molecules per [DEMA]-[OMs] ion pair (or that the water content was just less than 7000 ppm). The melting temperature for DEMA-OMs as received was measured by DSC to be 46 °C. The molecular structure of this ionic liquid is shown in Figure 2a.

2.3 Preparation of silica/DEMA-OMs gels

The nano-porous silica particles were first dehydrated at 200 °C for 5 hours in order to remove residual organic impurities from the synthesis as well as possibly adsorbed water. Since DEMA-OMs is solid at room temperature, a small amount of H_2O, namely at a molar ratio H_2O:DEMA-OMs equal to 0.22:1, was deliberately added to decrease the melting point to just below room temperature.[36] Then, a series of silica/DEMA-OMs composites (hereafter called gels) with a silica volume fraction, ΦSiO_2, equal to 0.00, 0.08, 0.12, 0.21, 0.35, 0.52 and 0.68, were prepared by dissolving calculated amounts of silica and ionic liquid in 0.5 or 1 ml of ethanol, Table 1. For every gel the pore filling factor, i.e. the percent of the available pore volume actually filled, is also given. The solution was stirred for 2 hours to achieve a homogeneous filling of the nano-pores, and then kept aside at room temperature for 24 hours to evaporate ethanol. The silica/DEMA-OMs gels were further dried at 80 °C for 20 hours to remove the remaining traces of ethanol. After these treatments the samples were sealed in NMR tubes (Figure 2b) and vials for NMR and Raman characterization, respectively.

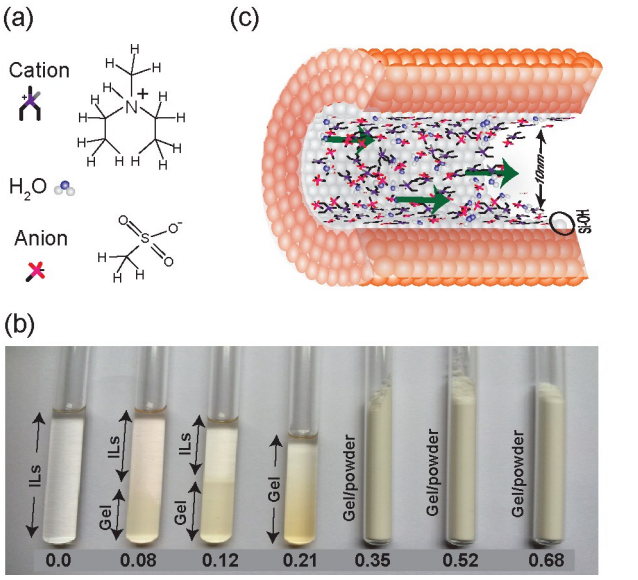

Fig. 2 Molecular structure of diethyl-methyl ammonium methanesulfonate, DEMA-OMs (a), and photo of the NMR tubes containing the silica gels with ΦSiO_2= 0–0.68 (b). A cartoon of the ionic liquid filled silica nano-pore is given in (c), with the Si-O-Si extended network represented in orange and the surface –SiOH groups in white. The average size of the pores is 10 nm.

Even the gels with the lowest filing factor, i.e. those where the ionic liquid only fills 25% of the available pore volume, show to be monophasic, that is the liquid is entirely incorporated into the pores and is not separated from the powder. Due to the structure of the silica particles, the surface area (338 m^2/g) is distributed as 5% outer surface and 95% inner or pore surface. Hence, if the added ionic liquid would not be inside the pores the material would look gelly-like rather than as a powder, as it in fact does, Figure 2b. As we will see later, solid-state NMR results also confirm that the ionic liquid is successfully immobilized inside the nano-pores. An illustration of the ionic liquid filled silica nano-pore is provided in Figure 2c.

Table 1. Composition of the gels prepared with different amounts of silica and ionic liquid.

Pore filling (%)	Volume fraction of silica (ΦSiO_2)	Silica (g)	DEMA-OMs (ml)	Ethanol (ml)
25	0.683	0.70	0.146	1.0
50	0.520	0.70	0.295	1.0
100	0.350	0.60	0.506	1.0
200	0.212	0.30	0.506	0.5
400	0.120	0.16	0.540	0.5
600	0.082	0.12	0.607	0.5

2.4 Nuclear magnetic resonance spectroscopy, NMR

Solid-state NMR. One-dimensional (1D) ^1H, ^{29}Si, and $^{29}Si\{^1H\}$ cross-polarization (CP), and two-dimensional (2D) $^{29}Si\{^1H\}$ hetero-nuclear correlation (HETCOR) NMR experiments were performed on a Varian Infinity NMR spectrometer at a magnetic field of 14.1 T, operating at Larmor frequencies of 600.12 MHz for ^1H and 120.28 MHz for ^{29}Si. 1D ^{29}Si magic angle spinning (MAS) NMR spectra were collected using a 90° pulse length of 3.3 μs, under the condition of spinal proton decoupling (at a nutation frequency of 90 kHz), with a recycling delay of 100 s. 1D $^{29}Si\{^1H\}$ CP-MAS NMR spectra were recorded by transferring polarization from ^1H to ^{29}Si nuclei *via* RAMP-CP in order to fulfil the Hartmann-Hahn condition, with a CP contact time of 5 ms. The spectra were collected over 1024 transients with 5 s of recycling delay. ^1H NMR spectra were collected at a MAS rate of 10 kHz over 16 transients with a recycling delay of 5 s. 2D $^{29}Si\{^1H\}$ HETCOR NMR experiments were performed by spinning the sample at 10 kHz under MAS, where the magnetization is transferred from ^1H to ^{29}Si using ramp CP with contact time of 2 ms through Hartmann-Hahn condition. The signal in ^1H dimension was accumulated for 96 t_1 increments, with 320 transients, and a repetition delay of 2 s. All NMR experiments were performed at room temperature. ^1H and ^{29}Si chemical shifts were externally referenced to a standard 3-(trimethylsilyl)propanoic acid (TMSP) at 0 ppm (^1H) and 1.5 ppm (^{29}Si) with respect to TMS.

PFG NMR. Pulsed field gradient (PFG) NMR experiments were performed on a Bruker AVANCE (III) NMR spectrometer, at a magnetic field of 14.1 T, equipped with a ^1H diffusion probe with a maximum field gradient strength of 1200 G/cm. The self-diffusion coefficients were measured at 25 °C using a bipolar field gradient (diffstebp) NMR pulse sequence.[38] This suppresses magnetic field susceptibilities induced at the silica/DEMA-OMs interface that would otherwise contribute to the overall self-diffusion values. During

the experiments the signal attenuation was achieved in 16 steps with 50 G/cm for each increment. ^{1}H T_1 and T_2 were measured separately to calibrate the recycling delay and small delta (δ), respectively. The self-diffusion coefficients were obtained using the Stejskal-Tanner equation:

$$I/I_0 = \exp[-(\gamma G\delta)^2 (\Delta-\delta/3)D] \quad (1)$$

where γ is the gyromagnetic ratio of ^{1}H, G is the gradient strength, δ and Δ are the time delays that correspond to gradient pulse width and diffusion time respectively, and D is the self-diffusion coefficient. Considering that the silica nano pores have an average size of 10 nm, and that under these experimental conditions we probe diffusion distances between 100 nm and a few μm, the measured D values represent an apparent self-diffusion where the molecular motion is restricted by the pore walls.

2.5 Raman spectroscopy

Raman spectra were collected on a Renishaw InVia Reflex spectrometer equipped with a CCD and using the 785 nm wavelength from a near infrared diode laser as the excitation source. The nominal spectral resolution using this monochromatic light and a 1200 l/mm grating was better than 1 cm^{-1}. When collecting Raman spectra the laser power was chosen to be 100 or 50% of its maximum value, which is 100 mW at the source. The Raman spectra of all silica/DEMA-OMs gels were collected at room temperature over 5 accumulations, each with 10 s of acquisition time.

3 Results and Discussion

3.1 Structure of nano-porous silica

The Raman spectrum of the as-prepared nano-porous silica micro-particles is shown in Figure 3 (blue trace). It reveals the typical signatures of amorphous silica with a dominant and broad intensity peak at 430 cm^{-1} and a sharper signature at 485 cm^{-1}, assigned to the Si-O-Si bending modes of the extended silica network (R modes) and of the 4-membered rings (D_1 modes), respectively.[39, 40] In addition, distinct Raman intensities are observed at 800 cm^{-1} and 980 cm^{-1}, attributed to symmetric Si-O-Si and Si-OH stretching modes. The relatively strong intensity of the vibrational mode at 980 cm^{-1} indicates that the surface of silica contains a considerable amount of silanol groups. This high concentration of surface –SiOH groups is further verified by the appearance of a signature at 605 cm^{-1} in the Raman spectrum after treatment at 400 °C (red trace). This new mode is attributed to the formation of 3-membered rings (D_2 modes) from the condensation of proximate –SiOH groups.[41, 42]

The structure of the silica micro-particles was further investigated by solid-state MAS NMR spectroscopy. The corresponding spectrum is shown in Figure 4a, revealing the presence of different Q^n ^{29}Si species, where n indicates the number of *Si*-(O-Si) bonds established by one single *Si* atom. The high intensity at -101.5 ppm is assigned to Q^3 species, or to $Si(\text{-}OSi)_3(OH)_1$ species, which confirms the presence of surface –SiOH groups. By contrast, Q^2 and Q^4 species are found at -90.5 and -111.5 ppm respectively. By a peak-fitting analysis of the spectrum (using Dmfit[43] model) we have quantified that nano-porous silica contains 79% of Q^4, 19% of Q^3, and only 2% of Q^2 ^{29}Si species. The relatively low fraction of partially condensed Q^n ^{29}Si species observed in the 1D quantitative ^{29}Si NMR spectrum is consistent with the BET results showing a specific surface area of 338 m^2/g.

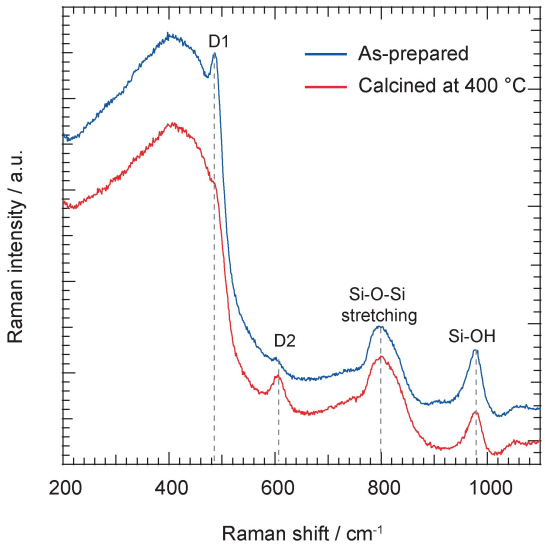

Fig 3. Raman spectra of the nano-porous silica micro-particles as prepared (blue), and after heat treatment at 400 °C (red).

3.2 Molecular proximity to the silica surface

To get a detailed picture of the local organization of the molecules at the silica-ionic liquid interface, 2D ^{29}Si{^{1}H} HETCOR solid-state NMR spectra were collected for the sample with the lowest ionic liquid content, i.e. for the gel with ΦSiO_2 = 0.68 or 25% of pore filling. These spectra allow probing the spatial proximity of the ^{29}Si and ^{1}H nuclei. Figure 4b shows the 2D pattern of the magnetization transfer from ^{1}H to ^{29}Si, with the corresponding correlation peaks that result from hetero-nuclear dipolar couplings between ^{29}Si and ^{1}H nuclei. ^{29}Si{^{1}H} CP MAS and ^{1}H MAS NMR spectra are shown on top and at left of this 2D spectrum, Figure 4c and 4d. The strongest correlation peak at ~5 ppm in the ^{1}H dimension correlates to different Q^n sites in the ^{29}Si dimension, and is assigned to H_2O molecules adsorbed on the silica surface. The presence of adsorbed water is expected considering the hydrophilic character of the gels, as well as the preparation procedure of the gels (see section 2.3). Although H_2O molecules are highly mobile in nature, this intense correlation peak indicates strong dipolar interactions between H_2O and Q^n ^{29}Si species in this gel and thus a reduced mobility.

An additional broad correlation peak is detected centered at ~7 ppm in the ^{1}H dimension, which correlates exclusively with the Q^3 ^{29}Si species, or surface silanol groups. Further correlation peaks are found in the 2–4 and 8–10 ppm shift ranges, demonstrating the molecular proximity of the ionic

liquid to the silica surface. While the proximity of the cation is implicitly given by the correlation peaks at 8.7 and 3.2 ppm assigned to the –NH and CH_2^{cation} groups, the proximity of the anion is more difficult to assess, due to the vicinity of the CH_3^{anion} and CH_3^{cation} chemical shifts. Overall, the less intense correlation peaks related to the ionic liquid compared to those assigned to water, suggest that the nano-confined cation:anion pairs are either more mobile (even at a pore filling of only 25%, or ΦSiO_2 = 0.68), or less proximate to the silica surface. Most likely, given the hydrophilic character of silica, water molecules constitute the first molecular layer adsorbed on silica. In support for this scenario is the observation that upon heat treatment at 150 °C for 24 hours the signature attributed to water in the 1D ^{1}H NMR spectrum vanishes, as well as the correlation peak associated to Q^n ^{29}Si sites in the 2D ^{29}Si{^{1}H} HETCOR spectrum, Figure SI1. Concomitantly, the intense correlation peaks persisting at ~6 ppm (surface silanol) and at 8.6 and 3.9 ppm (-NH and CH_2^{cation}) indicate that upon dehydration the ionic liquid comes closer to the silica surface. This is a further confirmation that the ionic liquid is successfully immobilised inside the silica nano-pores.

3.3 Inter-molecular interactions

In Figure 5, the ^{1}H MAS NMR spectra of the gels with an increasing silica volume fraction (ΦSiO_2) are shown. In the silica-free sample (ΦSiO_2 = 0), the presence of water is revealed by the ^{1}H chemical shift at 4.0 ppm, while the –NH proton of the DEMA cation is observed at 9.2 ppm. For an increasing volume fraction of silica (ΦSiO_2 = 0.21 – 0.68), the H_2O peak shifts down-field (from 4.0 to 4.9 ppm) while the –NH peak shifts up-field (from 9.2 to 8.6 ppm), see also Figure SI2. This trend for chemical shifts is similar to that recently observed upon addition of H_2O to DEMA-OMs,[36] and suggests that upon confinement the cationic –NH group experiences weaker interactions, oppositely to water.[36] It is also notable that the width of the water signal increases with the silica volume fraction despite the higher spinning rates, this increase being much more pronounced than for the peaks assigned to the ionic liquid, Figure SI3. This evidences that water molecules become less mobile than the ionic liquid, in agreement with the hypothesis expressed above that in the gel with ΦSiO_2 = 0.68 they constitute the first hydration layer on the silica surface. This can in turn indicate that water molecules establish stronger H-bonds with the surface –SiOH groups, as more silica surface is available. This scenario is consistent with the appearance of a broad peak resonating at ~7 ppm for samples with ΦSiO_2 = 0.35–0.68. Since the presence of water has an important effect on the ionic liquids' properties and these gels are of hydrophilic character, we have calculated from solid-state ^{1}H NMR integrated areas the exact amount of water actually present in the gels, which despite the precautions taken in the sample preparation is about two H_2O molecules per DEMA:OMs pair, Figure SI4a. This amount of water, higher than the one deliberately added during preparation, is plausibly absorbed from the atmosphere when transferring the samples from the sealed NMR tubes to the solid-state rotor. Interestingly, this ratio is constant in all the gels, which translates into a progressively lower amount of H_2O molecules when normalized to the available surface area, Figure SI4b. Hence, an important observation based on the full width at half maximum (FWHM) dependence of the chemical shift of water (Figure SI3) is that despite the same relative concentration with respect to the ionic liquid, the water absorbed by the liquid phase distributes in the gel differently depending on ΦSiO_2, and becomes more surface bound for lower pore filling factors. This is in agreement with the results presented by Milischuk *et al.*,[44] for the structure and dynamics of water in silica nano pores. These reveal a thin surface-bound layer of water with a different density, stronger H-bonds, a preferential orientation, and a significantly decreased mobility than water located at the pore centre.

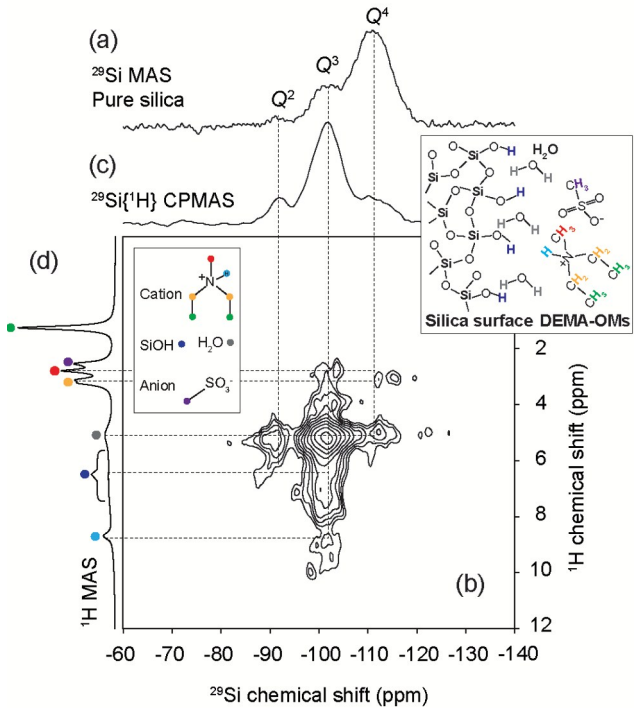

Fig. 4 (a) Quantitative ^{29}Si MAS, (b) 2D solid-state ^{29}Si{^{1}H} HETCOR with a lowest contour level of 23%, (c) ^{29}Si{^{1}H} CP-MAS, and (d) ^{1}H MAS NMR spectra of the silica/DEMA-OMs gel with ΦSiO_2 = 0.68, or 25% pore filling. NMR spectra were collected at a magnetic field of 14.1 T and a MAS rate of 10 kHz.

To achieve complementary information on the nature of intermolecular interactions established in the gels, we have employed Raman spectroscopy that, as compared to NMR spectroscopy, is weakly sensitive to the presence of water and silica. Hence, the signatures of both the DEMA cation and the OMs anion can be distinctively analysed with little interference from the other molecular species. Figure 6a (top trace) shows the Raman spectrum of a silica/DEMA-OMs gel with ΦSiO_2 = 0.68. The broad contribution underlying the sharper features in the low frequency range 200–500 cm^{-1} is attributed to the Si-O-Si bending modes typical of amorphous silica (bottom trace). Raman peaks at 340 and 554 cm^{-1} are attributed to S–O rocking

and bending modes, while the C-N-C and N-C-C bending modes are detected in the region 408–486 cm^{-1}.[45]

Two intense peaks at 748 and 1040 cm^{-1} are assigned to the C–S and S–O stretching modes of the anion, respectively.[32] Less intense peaks in the high frequency region from 2800 to 3050 cm^{-1} arise from C–H and N–H stretching modes with contributions from both the cation and the anion. In analyzing the Raman spectra of the gels, we have mainly focused on the S–O stretching vibrations, Figure SI5a, since these are very sensitive to inter-molecular interactions.[36] By a detailed peak-fit analysis, we find that the frequency of this stretching mode clearly increases with the silica content, Figure 6b, indicating a contraction of the S–O bond as a result of a new chemical environment for the OMs anion, different from pure anion–cation interactions.

Since the natural site for interaction on the counter-ion, *i.e.* the –NH group of the ammonium, shows to experience weaker interactions upon increasing silica content (Figure 5), we deduce that the Raman frequency increase shown in Figure 6b is due to a water-anion interaction established close to the silica surface (more details in next section). This is also consistent with the shift down-field of the ^1H signal of water shown in Figure 5. In support for this scenario is also the observation that all vibrations in the C–H and N–H stretching range 2700–3200 cm^{-1} attributed to the cation shift slightly to higher wavenumbers with increasing

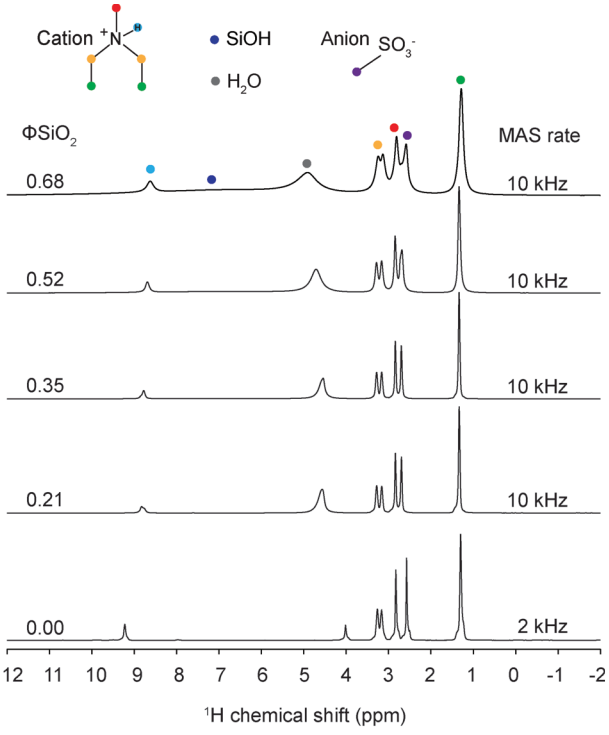

Fig. 5 ^1H solid-state MAS NMR spectra for silica/DEMA-OMs gels with ΦSiO_2 varying from 0 to 0.68 (from bottom to top). The samples were spun at a MAS rate of 10 kHz except for the silica free sample for which the spinning rate was 2 kHz. ^1H NMR spectra were acquired with 16 transients and 5 s recycling delay at room temperature.

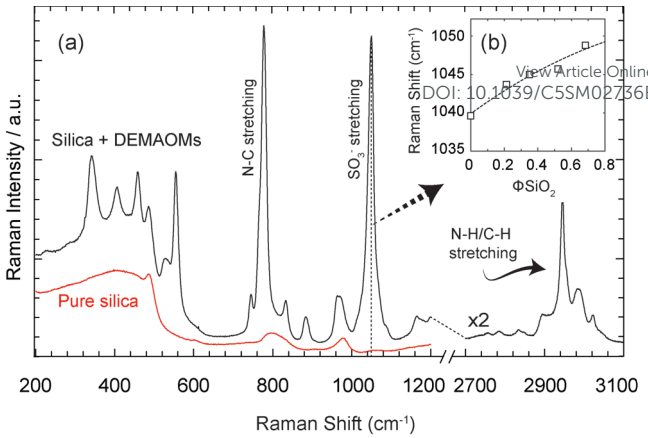

Fig. 6 (a) Raman spectrum of the silica/DEMA-OMs gel with ΦSiO_2 = 0.68, (b) frequency shift of the S–O stretching mode plotted as a function of the silica volume fraction ΦSiO_2.

silica content, indicating an overall weaker interaction of the ammonium cation with its chemical surrounding (Figure SI5b). Thus, the presence of the silica surface, through adsorbed water, has the overall effect to weaken the anion-cation association, as also recently observed for the simpler binary system based on DEMA-OMs and H_2O.[36]

3.4 Mobility and transport properties

To determine to what extent surface interactions affect the mobile nature of DEMA-OMs, ^1H NMR spectra were collected for a series of silica/DEMA-OMs gels (ΦSiO_2 = 0–0.68) at static conditions in a solution-state spectrometer, Figure 7a. The ^1H peaks become progressively broader upon confinement, and significantly so for a volume fraction of silica equal to 0.35, which corresponds to a 100% pore filling. This gel thus represents a threshold composition that reveals different natures of the ionic liquid. More specifically, for a pore filling larger than 100% there is ionic liquid also in the inter-particle space with a higher mobility, whereas for a pore filling smaller than 100% the ionic liquid is inside the nano-pores and displays a lower mobility. The gels with ΦSiO_2 = 0.35 and 0.68 have therefore been further investigated by collecting ^1H NMR spectra on a solid-state spectrometer with different MAS rates, Figure 7b and 7c respectively. Although the spectrum looks broad at 0 spinning rate, the lines are significantly narrowed already at 2 kHz, with no further increase in resolution for higher spinning rates. Since a spinning rate of 2 kHz is relatively low for the recovery of narrow lines, this behaviour suggests that despite the nano-confinement in the 10 nm sized domains and the establishment of interactions with the silica surface, the ionic liquid's mobility is only partially, and not drastically, affected. This conclusion is in qualitative agreement with the findings of Le Bideau *et al.*,[8, 26] who by performing ^1H MAS NMR and relaxation measurements found that the imidazolium ionic liquid $C_4C_1ImTFSI$ confined in monolithic silica within 15 nm large pores was only marginally slowed down.

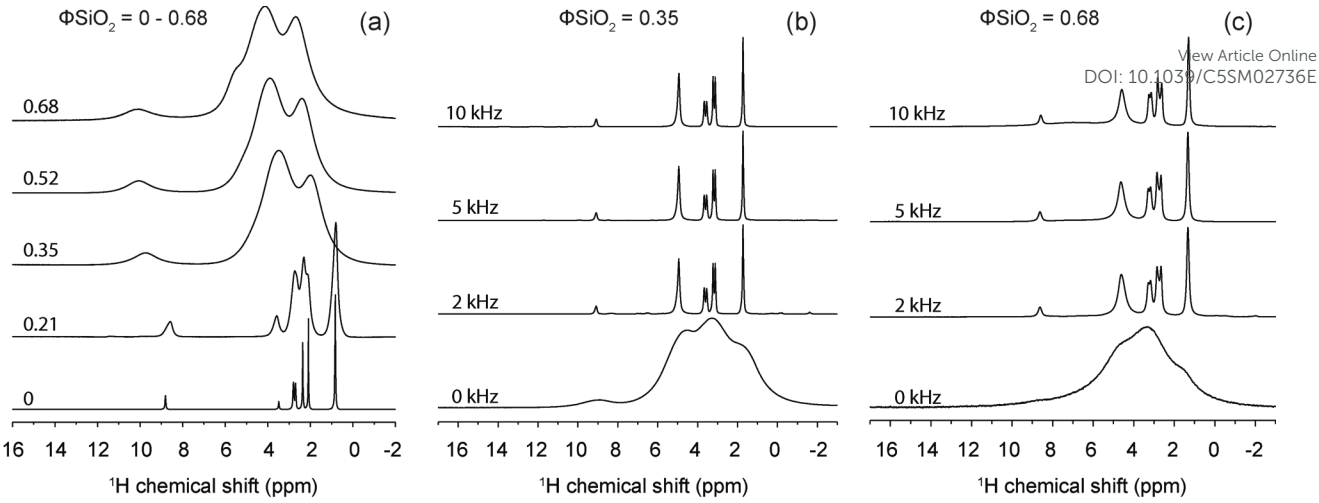

Fig. 7 ^{1}H NMR spectra of silica-ionic liquid composite with volume silica fraction (a) ΦSiO2 = 0 to 0.68, (b) ΦSiO2 = 0.35, (c) ΦSiO2 = 0.68. ^{1}H NMR spectra collected in a (a) 600 MHz solution-state NMR spectrometer at static conditions and (b, c) 600 MHz solid-state NMR spectrometer at a static condition and at MAS rate of 2, 5 and 10 kHz, respectively.

To achieve further insights on the effect of nano-confinement on the mobility of DEMA-OMs, we have measured the apparent self-diffusion coefficient (D) by ^{1}H PFG NMR spectroscopy, using a bipolar gradient pulse sequence[38] to eliminate susceptibility effects that can occur in heterogeneous materials. In Figure 8, the apparent self-diffusion coefficient of the cation (D^+) is shown for different volume fractions of silica (ΦSiO_2), as extracted from the ^{1}H signal at 1.3 ppm assigned to the CH_3 on the cation that is well separated from other peaks. One can note that diffusion values are not given for silica gels with ΦSiO_2<0.2, since these displayed phase separation (see also Figure 2b). Figure SI6 shows representative plots of I/I_0 vs G for pure DEMA-OMs and a silica gel. As expected D^+ decreases with ΦSiO_2, and reaches a plateau value at Φ=0.35 (or 100% of pore filling). As discussed in our previous work[12] the excluded volume effect alone would not be sufficient to describe the decrease in D in these kind of gels. Moreover, in these gels we have the concomitant and opposite effects of nano-confinement and water content. Hence, although we are confident that surface effects do play a role also in the gels investigated here, we cannot quantitatively distinguish between the retardation associated with direct surface effects[12] and an acceleration originating from the presence of water, even if at small content.[36] For comparison of the dependence on ΦSiO_2, in Figure 8 we also report the diffusion values previously measured by us for the imidazolium ionic liquid C_6C_1ImTFSI when confined in a silica gel prepared *via* a sol-gel route.[12] It is interesting to note that compared to the diffusion value at ΦSiO_2 = 0, the decrease is less severe in the gels investigate here. This may be rationalized by these gels having a lower surface area (338 m^2/g) than those prepared *via* the sol-gel synthesis (700–800 m^2/g),[12] and hence a weaker contribution from surface interactions for comparable SiO_2 volumes. Moreover, the fact that D does not decrease further for $\Phi SiO_2 \geq$ 0.35 in the gels here investigated may arise from the presence of water molecules and their tendency to polarize at the silica surface (as discussed above and suggested by Figure SI3). Interestingly this phenomenon has recently been theoretically predicted by molecular dynamics simulations of nano-confined water/ionic liquid mixtures.[46] When this occurs, potential surface effects that are otherwise associated to a dynamical retardation can be screened. Nevertheless, the less dramatic mobility loss that we observe in these gels, as compared to sol-gel based ionogels previously studied, is interesting in the viewpoint of a possible use in next-generation PEM fuel cells.

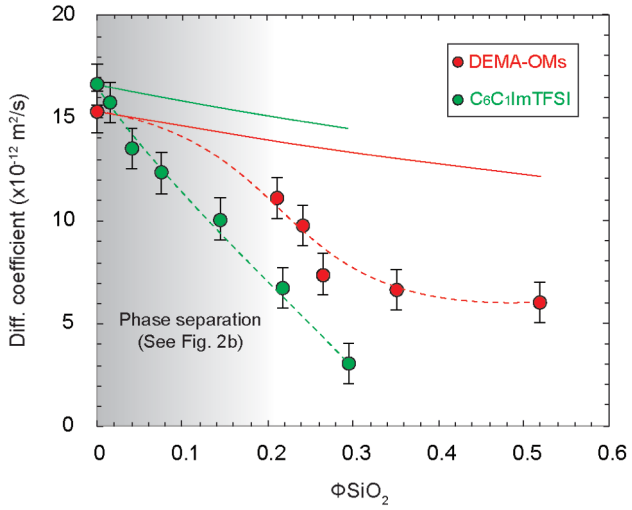

Fig. 8 Apparent self-diffusion coefficients of the DEMA cation in gels with increasing silica content (red circles). For comparison, the D values measured for an ionogel prepared *via* a sol-gel route and based on the imidazolium ionic liquid C_6C_1ImTFSI[12] are also shown (green circles). The dependence of D on the silica volume fraction ΦSiO_2 as theoretically expected from the excluded volume model, i.e. from the relation $D(\Phi) = D_{bulk}/(1+0.5\Phi)$ where D_{bulk} is the bulk diffusion coefficient is shown as a red and green solid line for the two types of gels, respectively. The dashed lines are just guides to the eye.

Table 2. Apparent self-diffusion coefficient (D) of the DEMA cation in silica gels with ΦSiO_2 = 0 – 0.52. For gels where a bi-exponential function is found, D_1 and D_2 are additionally given.

ΦSiO_2	Apparent self-diffusion coefficients, D [m^2/s]		
	D	D_1	D_2
0.00	$1.51 \cdot 10^{-11}$		
0.21	$1.11 \cdot 10^{-11}$	$1.71 \cdot 10^{-11}$	$7.33 \cdot 10^{-12}$
0.24	$9.75 \cdot 10^{-12}$	$1.30 \cdot 10^{-11}$	$5.48 \cdot 10^{-12}$
0.26	$7.38 \cdot 10^{-12}$	$1.01 \cdot 10^{-11}$	$4.28 \cdot 10^{-12}$
0.35	$6.62 \cdot 10^{-12}$		
0.52	$5.96 \cdot 10^{-12}$		

As a mean to elucidate further the nature of the diffusional motion, we have examined the dependence of $\ln(I/I_0)$ on $(\gamma G\delta)^2(\Delta-\delta/3)$, Figure SI7. For the silica free sample and for the gels with $\Phi SiO_2 \geq 0.35$ a single-exponential behaviour is observed, whereas for those with $\Phi SiO_2 < 0.35$ (that is for ΦSiO_2 = 0.21 or 200% pore filling; ΦSiO_2 = 0.24 or 170% pore filling; and ΦSiO_2 = 0.26 or 150% pore filling) a bi-exponential behaviour is observed, Table 2. Considering the values found for D_1 and D_2 (Table 2) this can be rationalized by distinguishing between the ionic liquid located in the inter-particle domains, that has a close to bulk-like behaviour with a slightly reduced mobility, and the ionic liquid located in the intra-particle domains, that is inside the nano-pores, that experiences the effects of nano-confinement and is thus much slower. This distinction is in agreement with the conclusions drawn from Figure 7a. From the D_1 and D_2 values one can calculate the relative population of the ionic liquid molecules residing in the inter- (χ^{inter}) and intra-particle (χ^{intra}) domains. For the case of the gel with ΦSiO_2=0.24 for example, we obtain that 43% of the IL resides inside the nanopores, which is in agreement with the stoichiometry of the synthesis.

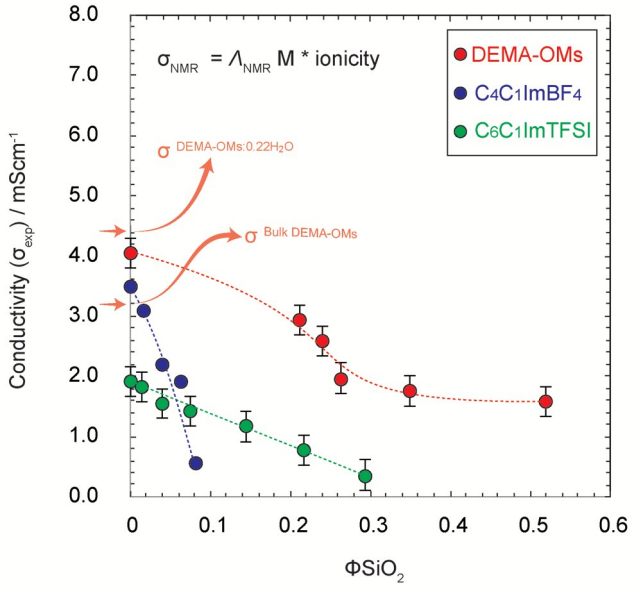

Fig. 9 Expected ionic conductivity calculated from the apparent self-diffusion coefficients and using the Nernst-Einstein relation (red circles). The ionic conductivity values reported for other silica gels based on the ionic liquid $C_4C_1ImBF_4$[50] (dark blue), and σ_{exp} values calculated for the ionogels based on $C_6C_1ImTFSI$[12] (green), are also shown for comparison. The dotted lines are just guides to the eye.

It should be stressed here that the diffusion values could not be estimated for gels with a silica volume fraction higher than 0.52 due to considerable peak broadening, nor for the anion due to overlap of the CH_3^{anion} signature. However, based on the recent results published by Yaghini et al.,[36] we can assume that the anion and the cation diffuse at the same rate. The diffusivity of H_2O is also challenging to measure especially for silica gels with ΦSiO_2>0.21 due to its broad signature. Nevertheless, the higher resolution of the H_2O peak in the samples with ΦSiO_2 = 0 and 0.21 allowed to estimate D^{H2O} to be 8.38×10^{-11} m^2/s (single exponential), and 6.96×10^{-11} and 1.28×10^{-11} m^2/s (bi-exponential), respectively. Hence, also for water, distinct diffusional properties are observed in the inter- and intra-particle regions.

Due to some previous results indicating that the D^+/D^- ratio changes significantly only for very high silica content[12] and that the D^+/D^- ratio for DEMA-OMs keeps constant and equal to 1 upon addition of water,[36] we express the hypothesis that in our gels $D^{DEMA} \approx D^{OMs}$ and that the ionicity of the ionic liquid, which is close to 0.6 in the bulk, is maintained in the gels. Based on this hypothesis, the expected ionic conductivity, σ_{exp}, calculated as $\sigma_{exp} = 0.6 \cdot \Lambda_{NMR} \cdot M$, where Λ_{NMR} is deduced from the Nernst-Einstein relation $\Lambda_{NMR}=(D^+ + D^-) \cdot F^2/RT$, M is the molarity of the DEMA-OMs/water liquid phase, F is the Faraday's constant, R is universal gas constant, T is the temperature and D^+ and D^- are the diffusion coefficients of the cation and the anion respectively, σ_{exp} falls in the range 1.6–4.1 mS/cm, Figure 9. The Λ_{NMR} values obtained from Nernst-Einstein relation are also given in Figure SI8. One should note that σ_{exp} so expressed takes only into account the concentration and mobility of the ionic species, but is not scaled to the volume fraction of the liquid phase actually present in the gel. Figure 9 shows that our values are comparable with those previously reported for other ionogels based on imidazolium ionic liquids.[14, 16, 47-50] However, compared to these other systems, the gels here investigated reveal a smoother decrease with ϕSiO_2 making them more competitive at higher silica contents, which may be needed for better mechanical properties. Another observation is that despite the slower self-diffusion as compared to, for instance, the gels based on $C_6C_1ImTFSI$, the expected conductivity is higher as a result of the higher molarity (M) of an ionic liquid based on smaller molecules, such as DEMA and OMs. It is also interesting to note that despite the similar preparation procedure of the gels shown in Figure 9 as green[12] and dark blue[50] circles, the latter shows a stronger dependence of conductivity on ϕSiO_2. Although the better performance of the gels based on DEMA-OMs can in part be explained by the presence of some water (as discussed above), a shift of the whole curve to the anhydrous

state (see point indicated as σ_{bulk} DEMA-OMs) would still correspond to higher ionic conductivities in the entire concentration range. Gels based on nano-porous silica micro-particles seem therefore to be promising for use as PEM materials in fuel cells, but can still be improved by choosing an ionic liquid with even higher bulk conductivity and/or by modification of the chemistry at the silica surface such that surface interactions are minimized. These approaches will be at focus in our next coming paper.

4 Conclusions

This work presents a comprehensive study of the local correlation and dynamics in a new type of gels based on nano-porous silica micro-particles filled with the protic ionic liquid DEMA-OMs. In these gels, a small amount of water is present due to a deliberate addition during the gel preparation. Our NMR results indicate that water molecules, when present, constitute the first adsorbed layer on silica and display a much lower mobility than they would do in the bulk. Water molecules also interfere with the native anion-cation interaction, as revealed by Raman spectroscopy. The 2D NMR correlation pattern indicates the vicinity of the DEMA cation (or its $-NH^+$ group) to the silica surface, which becomes even more evident upon dehydration of the gel. The proximity of the OMs anion is not as evident, which is likely due to the orientation of the $-SO_3^-$ group, rather than the $-CH_3$ towards the hydrated silica surface. However, the complex nature of intermolecular interactions in this new type of hybrid materials is such that the mobility of the ions is slightly but not dramatically affected by nano-confinement, which we attribute to a screening of surface effects by adsorbed water. In particular, the apparent self-diffusion coefficients are higher than those previously measured for gels based on imidazolium ionic liquids, and also show a smoother dependence on the volume fraction of silica (ΦSiO_2). The silica gel concept proposed here combines low surface area with high and well connected pore volume and extremely good mechanical strength, which makes it ideal for use in PEM Fuel Cells. In particular, compared to silica gels previously investigated, this is more competitive at higher silica volume fractions. These nano-porous silica micro-particles also offer the advantage of tunable pore size and pore morphology, as well as of a chemically modifiable surface area. The effect of surface modifications on the ionic liquid's dynamics will be the scope of the next study, whose results will be published in a separate paper. Ultimately, this unique type of silica micro-particles is not only interesting for energy applications, but can be exploited as a model system to investigate in more details the effect of nano-confinement on any other molecular liquid. This may be of relevance in any application where mass transport and controlled delivery are crucial aspects.

List of Symbols and Acronyms

G	Gradient strength / T m^{-1}
γ	Gyromagnetic ratio of ^1H / 10^6 rad s^{-1} T^{-1}
δ	Gradient pulse width / ms
Δ	Diffusion time / ms
D	Self-diffusion coefficient / m^2 s^{-1}
I	Signal intensity / a.u.
I_0	Signal intensity at zero gradient / a.u.
Λ_{NMR}	Molar conductivity calculated through Nernst-Einstein equation / S m^2mol^{-1}
σ_{exp}	Expected ionic conductivity calculated from Nernst-Einstein equation / mS cm^{-1}
F	Faraday's constant / s A mol^{-1}
R	Gas constant / J mol^{-1} K^{-1}
ΦSiO_2	Volume fraction of silica
DEMA-OMs	DiEthylMethylAmmoniumMethanesulfonate
$C_6C_1ImTFSI$	1-methyl-3-hexylimidazolium bis(trifluoromethanesulfonyl)imide
NMR	Nuclear magnetic resonance
PFG NMR	Pulsed field gradient NMR spectroscopy
FWHM	Full-Width at Half-Maximum
1D/2D	One-dimensional/Two-dimensional
CPMAS	Cross-Polarisation Magic Angle Spinning
RAMPCP	Ramped-Amplitude Cross-Polarization
HETCOR	HETeronuclear COrrelation
TMSP	3-(trimethylsilyl)propanoic acid
BET	Brunauer-Emmett-Teller
PEM	Proton Exchange Membrane
DSC	Differential Scanning Calorimetry
SEM	Scanning Electron Microscopy

Acknowledgements

The financial support from the Swedish Research Council (VR, grant no. 2012-3186), the Swedish Foundation for Strategic Research (SSF, grant no. ICA 10-0074) and from the Chalmers Areas of Advance *Energy* and *Materials Science* is kindly acknowledged. Finally, the Swedish NMR Centre at Gothenburg is greatly acknowledged for the use of spectrometers to perform solid-state and PFG NMR experiments.

References

1 H. Weingärtner, *Angewandte Chemie International Edition*, 2008, **47**, 654-670.
2 F. Shi, Q. Zhang, D. Li and Y. Deng, *Chemistry – A European Journal*, 2005, **11**, 5279-5288.
3 M. H. Valkenberg, C. DeCastro and W. F. Hölderich, *Green Chemistry*, 2002, **4**, 88-93.
4 L. Viau, C. Tourné-Péteilh, J. M. Devoisselle and A. Vioux, *Chemical Communications*, 2010, **46**, 228-230.
5 B. G. Trewyn, C. M. Whitman and V. S. Y. Lin, *Nano Letters*, 2004, **4**, 2139-2143.
6 I. F. Díaz-Ortega, J. Ballesta-Claver, M. Cruz Martín, S. Benítez-Aranda and L. F. Capitán-Vallvey, *RSC Advances*, 2014, **4**, 57235-57244.
7 M. Armand, F. Endres, D. R. MacFarlane, H. Ohno and B. Scrosati, *Nat Mater*, 2009, **8**, 621-629.
8 J. Le Bideau, L. Viau and A. Vioux, *Chemical Society Reviews*, 2011, **40**, 907-925.
9 M. P. Singh, R. K. Singh and S. Chandra, *Progress in Materials Science*, 2014, **64**, 73-120.
10 B. Lin, S. Cheng, L. Qiu, F. Yan, S. Shang and J. Lu, *Chemistry of Materials*, 2010, **22**, 1807-1813.
11 S. Dai, Y. H. Ju, H. J. Gao, J. S. Lin, S. J. Pennycook and C. E. Barnes, *Chemical Communications*, 2000, 243-244.

12 M. Nayeri, M. T. Aronson, D. Bernin, B. F. Chmelka and A. Martinelli, *Soft Matter*, 2014, **10**, 5618-5627.
13 R. Gobel, P. Hesemann, J. Weber, E. Moller, A. Friedrich, S. Beuermann and A. Taubert, *Physical Chemistry Chemical Physics*, 2009, **11**, 3653-3662.
14 M.-A. Néouze, J. L. Bideau, P. Gaveau, S. Bellayer and A. Vioux, *Chemistry of Materials*, 2006, **18**, 3931-3936.
15 M. A. B. H. Susan, T. Kaneko, A. Noda and M. Watanabe, *Journal of the American Chemical Society*, 2005, **127**, 4976-4983.
16 A. I. Horowitz and M. J. Panzer, *Journal of Materials Chemistry*, 2012, **22**, 16534-16539.
17 K. Ueno, K. Hata, T. Katakabe, M. Kondoh and M. Watanabe, *Journal of Physical Chemistry B*, 2008, **112**, 9013-9019.
18 T. Mizumo, T. Watanabe and H. Ohno, *Polym. J*, 2008, **40**, 1099-1104.
19 S. Shimano, H. Zhou and I. Honma, *Chemistry of Materials*, 2007, **19**, 5216-5221.
20 A. K. Mishra, T. Kuila, D. Y. Kim, N. H. Kim and J. H. Lee, *Journal of Materials Chemistry*, 2012, **22**, 24366-24372.
21 C. Iacob, J. R. Sangoro, P. Papadopoulos, T. Schubert, S. Naumov, R. Valiullin, J. Karger and F. Kremer, *Physical Chemistry Chemical Physics*, 2010, **12**, 13798-13803.
22 K. S. Han, X. Wang, S. Dai and E. W. Hagaman, *The Journal of Physical Chemistry C*, 2013, **117**, 15754-15762.
23 B. Coasne, L. Viau and A. Vioux, *The Journal of Physical Chemistry Letters*, 2011, **2**, 1150-1154.
24 G. Ori, F. Villemot, L. Viau, A. Vioux and B. Coasne, *Molecular Physics*, 2014, **112**, 1350-1361.
25 A. Martinelli, *European Journal of Inorganic Chemistry*, 2015, **2015**, 1300-1308.
26 J. Le Bideau, P. Gaveau, S. Bellayer, M. A. Neouze and A. Vioux, *Physical Chemistry Chemical Physics*, 2007, **9**, 5419-5422.
27 C. Iacob, J. R. Sangoro, W. K. Kipnusu, R. Valiullin, J. Karger and F. Kremer, *Soft Matter*, 2012, **8**, 289-293.
28 H. Song, Z. Luo, H. Zhao, S. Luo, X. Wu, J. Gao and Z. Wang, *RSC Advances*, 2013, **3**, 11665-11675.
29 M. P. Singh, R. K. Singh and S. Chandra, *Journal of Physical Chemistry B*, 2011, **115**, 7505-7514.
30 R. Göbel, A. Friedrich and A. Taubert, *Dalton Transactions*, 2010, **39**, 603-611.
31 J. Rodriguez, M. D. Elola and D. Laria, *The Journal of Physical Chemistry C*, 2012, **116**, 5394-5400.
32 E. Davies, Y. Huang, J. B. Harper, J. M. Hook, D. S. Thomas, I. M. Burgar and P. J. Lillford, *International Journal of Food Science and Technology*, 2010, **45**, 2502-2507.
33 P. V. Kortunov and V. D. Skirda, *Colloid Journal*, 2005, **67**, 573-580.
34 S. R. Veith, E. Hughes, G. Vuataz and S. E. Pratsinis, *Journal of Colloid and Interface Science*, 2004, **274**, 216-228.
35 M. Cifelli, V. Domenici, B. B. Kharkov and S. V. Dvinskikh, *Molecular Crystals and Liquid Crystals*, 2015, **614**, 30-38.
36 N. Yaghini, M. N. Garaga and A. Martinelli, *Fuel Cells*, 2015, doi: 10.1002/fuce.201500064.
37 N. Andersson, B. Kronberg, R. Corkery and P. Alberius, *Langmuir*, 2007, **23**, 1459-1464.
38 R. M. Corns, M. J. R. Hoch, T. Sun and J. T. Markert, *Journal of Magnetic Resonance (1969)*, 1989, **83**, 252-266.
39 A. Martinelli, *International Journal of Molecular Sciences*, 2014, **15**, 6488-6503.
40 B. Hehlen, *Journal of Physics Condensed Matter*, 2010, **22**.
41 B. Humbert, A. Burneau, J. P. Gallas and J. C. Lavalley, *Journal of Non-Crystalline Solids*, 1992, **143**, 75-83.
42 G. N. Papatheodorou and A. G. Kalampounias, *Journal of Physics Condensed Matter*, 2009, **21**.
43 D. Massiot, F. Fayon, M. Capron, I. King, S. Le Calvé, B. Alonso, J.-O. Durand, B. Bujoli, Z. Gan and G. Hoatson, *Magnetic Resonance in Chemistry*, 2002, **40**, 70-76.
44 A. A. Milischuk and B. M. Ladanyi, *Journal of Chemical Physics*, 2011, **135**.
45 F. E. Genceli Guner, M. Lutz, T. Sakurai, A. L. Spek and T. Hondoh, *Crystal Growth & Design*, 2010, **10**, 4327-4333.
46 Personal communication from Prof. Luis Miguel Varela Cabo.
47 Y.-S. Ye, G.-W. Liang, B.-H. Chen, W.-C. Shen, C.-Y. Tseng, M.-Y. Cheng, J. Rick, Y.-J. Huang, F.-C. Chang and B.-J. Hwang, *Journal of Power Sources*, 2011, **196**, 5408-5415.
48 E. Delahaye, R. Gobel, R. Lobbicke, R. Guillot, C. Sieber and A. Taubert, *Journal of Materials Chemistry*, 2012, **22**, 17140-17146.
49 A. I. Horowitz and M. J. Panzer, *Angewandte Chemie - International Edition*, 2014, **53**, 9780-9783.
50 S. A. M. Noor, P. M. Bayley, M. Forsyth and D. R. MacFarlane, *Electrochimica Acta*, 2013, **91**, 219-226.

View Article Online
DOI: 10.1039/C5SM02736E

View Article Online
DOI: 10.1039/C5SM02736E

TOC.

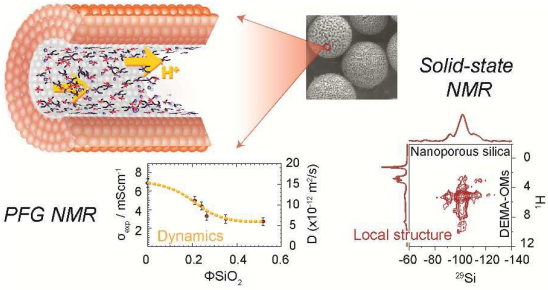

Local coordination and dynamics of a protic ionic liquid confined in nano-porous silica microparticles studied by Raman and NMR spectroscopy.